Instanton-Sphaleron transition in the d = 2 Abelian-Higgs model on a Circle

D.K. Park[1,2*], H. J. W. Müller-Kirsten[1†], J.–Q. Liang[1,3‡] and A. V. Shurgaia [1§]

1. Department of Physics, University of Kaiserslautern, D-67653 Kaiserslautern, Germany

2.Department of Physics, Kyungnam University, Masan, 631-701, Korea

3. Department of Physics and Institute of Theoretical Physics, Shanxi University, Taiyuan, Shanxi 030006, China

Abstract

The transition from the instanton–dominated quantum regime to the sphaleron–dominated classical regime is studied in the $d = 2$ abelian–Higgs model when the spatial coordinate is compactified to S^1. Contrary to the noncompactified case, this model allows both sharp first–order and smooth second–order transitions depending on the size of the circle. This finding may make the model a useful toy model for the analysis of baryon number violating processes.

*e-mail: dkpark@hep.kyungnam.ac.kr

†e-mail: mueller1@physik.uni-kl.de

‡e-mail:jqliang@mail.sxu.edu.cn

§email: shurgaia@physik.uni–kl.de

After the sphaleron solution in the Weinberg–Salam model had been found [1,2], the temperature dependence of baryon number violating processes (BNVP) was studied extensively. To understand the overall features of BNVP over the entire range of temperature, the computation of periodic instantons [3] and their corresponding classical actions is required. However, the calculation of these in the Weinberg–Salam model is a highly non–trivial problem, even if numerical techniques are employed. Hence in many cases simple toy models were used to explore the temperature dependence of BNVP.

An immediate candidate as a simple toy model is the $d = 2$ Mottola–Wipf(MW) model [4], which shares many common features with $d = 4$ electroweak theory. The scale invariance of the nonlinear $O(3)$ model is broken in the MW model by adding an explicit mass term. This has a close analogy to the fact that the conformal invariance of the electroweak theory is broken in the Higgs sector. Also, neither model supports a vacuum instanton which gives a dominant contribution to the winding number transition at low temperature. The transition between thermally assisted quantum tunneling dominated by periodic instantons and the classical crossover dominated by the sphaleron in the MW model has been analyzed in Refs. [5,6] and it has been shown that the instanton–sphaleron transition is of the sharp first–order type in the full range of parameter space.

Recently, however, a numerical study [7,8] of the $d = 4$ SU(2)–Higgs model – which is a bosonic sector of the electroweak theory – has shown that a smooth second–order transition occurs when $6.665 < M_H/M_W < 12.03$ although the first–order transition occurs when $M_H/M_W < 6.665$. This implies that the MW model does not exhibit a proper transition of BNVP when heavy Higgss are involved.

Another candidate as a toy model is the $d = 2$ abelian-Higgs model which supports vortex solutions [9], in particular the vacuum instanton and the sphaleron [10] simultaneously. The simultaneous existence of instanton and sphaleron causes the model to yield phase diagrams for the instanton–sphaleron transition which are completely different from those of electroweak theory, as shown in Ref. [11]. Furthermore, numerical [12] and analytical [13] approaches have shown that the instanton–sphaleron transition in this model is always of the

second-order type, regardless of the ratio M_H/M_W. Hence, contrary to the MW model, the abelian–Higgs model does not describe the instanton–sphaleron transition of the electroweak theory properly when the Higgs mass is small.

In the following we study the instanton–sphaleron transition in the $d = 2$ abelian-Higgs model when the spatial coordinate is compactified to S^1. Since, to our knowledge, the effect of the compactification of the spatial coordinate of this model has not yet been investigated, this is of interest on its own. Furthermore, we will show that this model exhibits both first–order and second–order transitions depending on the size of the circumference of the spatial coordinate domain. This means that the abelian–Higgs model defined on a circle can be a better toy model than the MW model or the uncompactified abelian-Higgs model for the analysis of BNVP.

We begin with the Euclidean action

$$S_E^{(0)} = \int d\tau dx \left[\frac{1}{4} F_{\mu\nu} F_{\mu\nu} + (D_\mu \phi)^* D_\mu \phi + \lambda [\mid \phi \mid^2 - \frac{v^2}{2}]^2 \right] \tag{1}$$

and its field equations

$$\begin{aligned} \partial_\mu F_{\mu\nu} &= ig \left[\phi^* (D_\nu \phi) - (D_\nu \phi)^* \phi \right], \\ D_\mu D_\mu \phi &= 2\lambda \phi (\mid \phi \mid^2 - \frac{v^2}{2}), \end{aligned} \tag{2}$$

where $D_\mu = \partial_\mu - igA_\mu$. We define as mass–dimensional parameters

$$\begin{aligned} M_H &\equiv \sqrt{2\lambda} v, \\ M_W &\equiv gv, \end{aligned} \tag{3}$$

which correspond to Higgs mass and gauge particle mass in electroweak theory respectively. It is easy to show that the static sphaleron solution in the $A_0 = 0$ gauge is given by

$$\begin{aligned} A_1 &= A = const, \\ \phi_{sph} &= \frac{kb(k)}{\sqrt{\lambda}} e^{igAx} sn[b(k)x], \end{aligned} \tag{4}$$

where $sn[z]$ is a Jacobian elliptic function, k is the modulus of the elliptic function, and

$$b(k) = \sqrt{\frac{\lambda}{2}} v \left(\frac{2}{1+k^2}\right)^{\frac{1}{2}}. \tag{5}$$

Since $sn[z]$ has period $4K(k)$, where $K(k)$ is the complete elliptic integral of the first kind, the circumference L of S^1 is defined by

$$L_n = \frac{4nK(k)}{b(k)}, \qquad\qquad n = 1, 2, 3 \cdots. \tag{6}$$

Since the transition rate is negligible for large n [14], we confine ourselves to the $L = L_1$ case in this paper.

In order to examine the type of instanton–sphaleron transition we have to introduce the fluctuation fields around the sphaleron and expand the field equations (2) up to the third order in these fields. If, however, one expands Eq.(2) naively, one will realize that the fluctuation operators are not diagonalized and, hence, the computation of the spectra of these operators becomes a very non–trivial problem. To avoid this difficulty, we choose the R_ξ gauge [15] by adding to the original action (1) the gauge fixing term

$$S_{gf} = \frac{1}{2\xi} \int d\tau dx \left[\partial_\mu A_\mu + \frac{ig}{2}\xi(\phi^2 - \phi^{*2})\right]^2. \tag{7}$$

Then the field equations for the total Euclidean action $S_E = S_E^{(0)} + S_{gf}$ become

$$\begin{aligned} \partial_\mu F_{\mu\nu} + \frac{1}{\xi}\left[\partial_\mu\partial_\nu A_\mu + ig\xi(\phi\partial_\nu\phi - \phi^*\partial_\nu\phi^*)\right] &= ig\left[\phi^*(D_\nu\phi) - (D_\nu\phi)^*\phi\right], \\ D_\mu D_\mu\phi + ig\phi^*\left[\partial_\mu A_\mu + \frac{ig\xi}{2}(\phi^2 - \phi^{*2})\right] &= 2\lambda\phi(\mid\phi\mid^2 - \frac{v^2}{2}). \end{aligned} \tag{8}$$

One can show directly that the sphaleron in this gauge is the same as that of Eq.(4) if $A = 0$:

$$\begin{aligned} A_1 &= 0, \\ \phi_{sph} &= \frac{kb(k)}{\sqrt{\lambda}} sn[b(k)x]. \end{aligned} \tag{9}$$

We now introduce the fluctuation fields around the sphaleron as follows:

$$\begin{aligned} A_0(\tau, x) &= a_0(\tau, x), \\ A_1(\tau, x) &= a_1(\tau, x), \\ \phi(\tau, x) &= \phi_{sph}(x) + \frac{1}{\sqrt{2}}\Big(\eta_1(\tau, x) + i\eta_2(\tau, x)\Big), \end{aligned} \tag{10}$$

where a_0, a_1, η_1, and η_2 are real fields. Inserting (10) into Eq.(1) and Eq.(7) one can express S_E for $\xi = 1$ as

$$S_E = \frac{E_{sph}}{T} + S_2 + S_3 + S_4 \tag{11}$$

where $1/T$ is the period of the sphaleron [16] and

$$\begin{aligned}
E_{sph} = \sqrt{2\lambda}v^3\Bigg[& \left[\left(\frac{2}{1+k^2}\right)^{-\frac{1}{2}} + \frac{1+2k^2}{3}\left(\frac{2}{1+k^2}\right)^{\frac{3}{2}} - 2\left(\frac{2}{1+k^2}\right)^{\frac{1}{2}} \right] K(k) \\
& + \left[2\left(\frac{2}{1+k^2}\right)^{\frac{1}{2}} - \frac{1+k^2}{3}\left(\frac{2}{1+k^2}\right)^{\frac{3}{2}} \right] E(k) \Bigg],
\end{aligned} \tag{12}$$

$$\begin{aligned}
S_2 = \int d\tau dx \Bigg[& \frac{1}{2}a_0[-\partial_\mu\partial_\mu + 2g^2\phi_{sph}^2]a_0 + \frac{1}{2}a_1[-\partial_\mu\partial_\mu + 2g^2\phi_{sph}^2]a_1 \\
& + \frac{1}{2}\eta_1\left[-\partial_\mu\partial_\mu + 2\lambda(3\phi_{sph}^2 - \frac{v^2}{2})\right]\eta_1 + \frac{1}{2}\eta_2\left[-\partial_\mu\partial_\mu + 2(\lambda+g^2)\phi_{sph}^2 - \lambda v^2\right]\eta_2 \\
& + 2\sqrt{2}g\phi'_{sph}a_1\eta_2 \Bigg],
\end{aligned}$$

$$\begin{aligned}
S_3 = \int d\tau dx \Bigg[& 2g(a_0\dot{\eta_1}\eta_2 + a_1\eta_1'\eta_2) + \sqrt{2}g^2\phi_{sph}(a_0^2 + a_1^2)\eta_1 \\
& + \sqrt{2}\lambda\phi_{sph}\eta_1^3 + \sqrt{2}(\lambda+g^2)\phi_{sph}\eta_1\eta_2^2 \Bigg],
\end{aligned}$$

$$S_4 = \int d\tau dx \left[\frac{g^2}{2}(a_0^2 + a_1^2)(\eta_1^2 + \eta_2^2) + \frac{\lambda}{4}(\eta_1^2 + \eta_2^2)^2 + \frac{g^2}{2}\eta_1^2\eta_2^2 \right],$$

where $E(k)$ is the complete elliptic integral of the second kind. Here the dot and the prime denote differentiation with respect to τ and x respectively. Due to the final term in S_2 the fluctuation operators for a_1 and η_2 are not diagonalized although the $R_{\xi=1}$ gauge has been chosen. To guarantee the diagonalization we introduce the fluctuation fields $\rho_\pm$ defined as

$$\begin{aligned}
\rho_+ &= v_1 a_1 + v_2\eta_2, \\
\rho_- &= -v_2 a_1 + v_1\eta_2,
\end{aligned} \tag{13}$$

where

$$\begin{aligned}
v_1 &= \sqrt{\frac{1 - (\phi_{sph}^2 - \frac{v^2}{2})f_1^{-\frac{1}{2}}}{2}}, \\
v_2 &= \sqrt{\frac{1 + (\phi_{sph}^2 - \frac{v^2}{2})f_1^{-\frac{1}{2}}}{2}},
\end{aligned} \tag{14}$$

and

$$f_1 = (\phi_{sph}^2 - \frac{v^2}{2})^2 \cosh^2\alpha - \frac{v^4}{4}\left(\frac{1-k^2}{1+k^2}\right)\sinh^2\alpha. \tag{15}$$

Here $\alpha = \sinh^{-1} 2\theta$ and θ is the dimensionless parameter

$$\theta \equiv \frac{2M_W}{M_H} = \sqrt{\frac{2g^2}{\lambda}}. \tag{16}$$

Using the field redefinition (13) and the first–order differential equation for ϕ_{sph},

$$\phi'_{sph} + \sqrt{\lambda}\left[\frac{v^4}{4}\left(\frac{2k}{1+k^2}\right)^2 - v^2\phi_{sph}^2 + \phi_{sph}^4\right]^{\frac{1}{2}} = 0, \tag{17}$$

it is straightforward to show that S_2 becomes

$$S_2 = \frac{1}{2}\int d\tau dx [a_0 D_0 a_0 + \eta_1 D_1 \eta_1 + \rho_+ D_+ \rho_+ + \rho_- D_- \rho_-], \tag{18}$$

where

$$\begin{aligned} D_0 &= -\partial_\mu\partial_\mu + 2g^2\phi_{sph}^2, \\ D_1 &= -\partial_\mu\partial_\mu + 2\lambda(3\phi_{sph}^2 - \frac{v^2}{2}), \\ D_\pm &= -\partial_\mu\partial_\mu + 2g^2\phi_{sph}^2 + \lambda(\phi_{sph}^2 - \frac{v^2}{2}) \mp \lambda\sqrt{f_1}. \end{aligned} \tag{19}$$

After inserting the field redefinition (13) into S_3 and also into S_4, one can derive the field equations for the fluctuation fields by varying the total action S_E, i.e.

$$\hat{l}\begin{pmatrix} a_0 \\ \rho_+ \\ \rho_- \\ \eta_1 \end{pmatrix} = \hat{h}\begin{pmatrix} a_0 \\ \rho_+ \\ \rho_- \\ \eta_1 \end{pmatrix} + \begin{pmatrix} G_2^{a_0} \\ G_2^{\rho_+} \\ G_2^{\rho_-} \\ G_2^{\eta_1} \end{pmatrix} + \begin{pmatrix} G_3^{a_0} \\ G_3^{\rho_+} \\ G_3^{\rho_-} \\ G_3^{\eta_1} \end{pmatrix}, \tag{20}$$

where

$$\hat{l} = \begin{pmatrix} \frac{\partial^2}{\partial z_0^2} & 0 & 0 & 0 \\ 0 & \frac{\partial^2}{\partial z_0^2} & 0 & 0 \\ 0 & 0 & \frac{\partial^2}{\partial z_0^2} & 0 \\ 0 & 0 & 0 & \frac{\partial^2}{\partial z_0^2} \end{pmatrix}, \qquad \hat{h} = \begin{pmatrix} \hat{h}_{a_0} & 0 & 0 & 0 \\ 0 & \hat{h}_{\rho_+} & 0 & 0 \\ 0 & 0 & \hat{h}_{\rho_-} & 0 \\ 0 & 0 & 0 & \hat{h}_{\eta_1} \end{pmatrix},$$

$$
\begin{aligned}
G_2^{a_0} &= \frac{2g}{b(k)}(v_2\rho_+ + v_1\rho_-)\dot{\eta_1} + \frac{2\sqrt{2}g^2}{b^2(k)}\phi_{sph}a_0\eta_1, \qquad (21)\\
G_3^{a_0} &= \frac{g^2}{b^2(k)}a_0\left[\eta_1^2 + (v_2\rho_+ + v_1\rho_-)^2\right],\\
G_2^{\rho+} &= \frac{2g}{b(k)}[v_2a_0\dot{\eta_1} + (v_1^2 - v_2^2)\rho_-\eta_1' + 2v_1v_2\rho_+\eta_1'],\\
&\quad + \frac{2\sqrt{2}\lambda}{b^2(k)}\phi_{sph}[v_2^2\rho_+\eta_1 + v_1v_2\rho_-\eta_1] + \frac{2\sqrt{2}g^2}{b^2(k)}\phi_{sph}\rho_+\eta_1,\\
G_3^{\rho+} &= \frac{g^2}{b^2(k)}\Bigg[\rho_+\eta_1^2 + v_2^2a_0^2\rho_+ + v_1v_2a_0^2\rho_- + 2v_1^2v_2^2\rho_+^3 + 3v_1v_2(v_1^2 - v_2^2)\rho_+^2\rho_-\\
&\qquad\qquad + (v_1^4 - 4v_1^2v_2^2 + v_2^4)\rho_+\rho_-^2 - v_1v_2(v_1^2 - v_2^2)\rho_-^3\Bigg]\\
&\quad + \frac{\lambda}{b^2(k)}\left[v_2^2\rho_+\eta_1^2 + v_1v_2\rho_-\eta_1^2 + v_2^4\rho_+^3 + 3v_1v_2^3\rho_+^2\rho_- + 3v_1^2v_2^2\rho_+\rho_-^2 + v_1^3v_2\rho_-^3\right],\\
G_2^{\rho-} &= \frac{2g}{b(k)}[v_1a_0\dot{\eta_1} + (v_1^2 - v_2^2)\rho_+\eta_1' - 2v_1v_2\rho_-\eta_1']\\
&\quad + \frac{2\sqrt{2}\lambda}{b^2(k)}\phi_{sph}[v_1^2\rho_-\eta_1 + v_1v_2\rho_+\eta_1] + \frac{2\sqrt{2}g^2}{b^2(k)}\phi_{sph}\rho_-\eta_1,\\
G_3^{\rho-} &= \frac{g^2}{b^2(k)}\Bigg[\rho_-\eta_1^2 + v_1^2a_0^2\rho_- + v_1v_2a_0^2\rho_+ + 2v_1^2v_2^2\rho_-^3 + v_1v_2(v_1^2 - v_2^2)\rho_+^3\\
&\qquad\qquad + (v_1^4 - 4v_1^2v_2^2 + v_2^4)\rho_+^2\rho_- - 3v_1v_2(v_1^2 - v_2^2)\rho_+\rho_-^2\Bigg]\\
&\quad + \frac{\lambda}{b^2(k)}\left[v_1^2\rho_-\eta_1^2 + v_1v_2\rho_+\eta_1^2 + v_1^4\rho_-^3 + v_1v_2^3\rho_+^3 + 3v_1^2v_2^2\rho_+^2\rho_- + 3v_1^3v_2\rho_+\rho_-^2\right],\\
G_2^{\eta_1} &= -\frac{2g}{b(k)}\Bigg[v_2(\dot{a_0}\rho_+ + a_0\dot{\rho_+}) + v_1(\dot{a_0}\rho_- + a_0\dot{\rho_-}) + 2(v_1v_1' - v_2v_2')\rho_+\rho_-\\
&\quad + (v_1^2 - v_2^2)(\rho_+'\rho_- + \rho_+\rho_-') + v_1'v_2(\rho_+^2 - \rho_-^2) + v_1v_2'(\rho_+^2 - \rho_-^2) + 2v_1v_2(\rho_+\rho_+' - \rho_-\rho_-')\Bigg]\\
&\quad + \frac{\sqrt{2}\lambda}{b^2(k)}\phi_{sph}(3\eta_1^2 + v_2^2\rho_+^2 + v_1^2\rho_-^2 + 2v_1v_2\rho_+\rho_-) + \frac{\sqrt{2}g^2}{b^2(k)}\phi_{sph}(a_0^2 + \rho_+^2 + \rho_-^2),\\
G_3^{\eta_1} &= \frac{g^2}{b^2(k)}(a_0^2 + \rho_+^2 + \rho_-^2)\eta_1 + \frac{\lambda}{b^2(k)}[\eta_1^3 + (v_2\rho_+ + v_1\rho_-)^2\eta_1].
\end{aligned}
$$

Here $z_0 \equiv b(k)\tau$, $z_1 \equiv b(k)x$, and the dot and the prime denote differentiation with respect to z_0 and z_1 respectively. Also, the fluctuation operators $\hat{h}_{a_0}$, $\hat{h}_{\rho_+}$, $\hat{h}_{\rho_-}$, and $\hat{h}_{\eta_1}$ are

$$
\begin{aligned}
\hat{h}_{a_0} &= -\frac{\partial^2}{\partial z_1^2} + \frac{2g^2}{b^2(k)}\phi_{sph}^2, \qquad (22)\\
\hat{h}_{\rho_+} &= -\frac{\partial^2}{\partial z_1^2} + \frac{1}{b^2(k)}\left[2g^2\phi_{sph}^2 + \lambda(\phi_{sph}^2 - \frac{v^2}{2}) + \lambda\sqrt{f_1}\right],
\end{aligned}
$$

$$\hat{h}_{\rho_-} = -\frac{\partial^2}{\partial z_1^2} + \frac{1}{b^2(k)}\left[2g^2\phi_{sph}^2 + \lambda(\phi_{sph}^2 - \frac{v^2}{2}) - \lambda\sqrt{f_1}\right],$$
$$\hat{h}_{\eta_1} = -\frac{\partial^2}{\partial z_1^2} + \frac{2\lambda}{b^2(k)}\left[3\phi_{sph}^2 - \frac{v^2}{2}\right].$$

The lowest few eigenvalues of $\hat{h}_{a_0}$ and $\hat{h}_{\eta_1}$ can be obtained exactly by using Lam$\acute{e}$'s equation [17]. It is easy to show that the spectrum of $\hat{h}_{a_0}$ consists of only positive modes whose explicit forms are not needed here for further study. Also, of the lowest eigenstates of $\hat{h}_{\eta_1}$, we need only the $2K$–antiperiodic eigenfunctions to recover the proper uncompactified limit as shown in Ref. [18]. The lowest two $2K$–antiperiodic eigenstates of $\hat{h}_{\eta_1}$ are summarized in Table I. It may be impossible to obtain the higher states analytically at present. Using $\int_{-K}^{K} \psi_i^{(\eta_1)*}\psi_j^{(\eta_1)}dz_1 = \delta_{ij}$, one can show that the normalization constant N_1 in Table I is given by

$$N_1 = \sqrt{\frac{3k^2}{2[(1-k^2)K - (1-2k^2)E]}}. \tag{23}$$

We now consider the eigenstates of $\hat{h}_{\rho_+}$ and $\hat{h}_{\rho_-}$. In Appendix A we explain how the eigenstates of $\hat{h}_{\rho_+}$ and $\hat{h}_{\rho_-}$ are computed numerically. Following the method of Appendix A, one can show that the eigenstates of $\hat{h}_{\rho_+}$ also consist of only positive modes which we do not need. What we need, is only the negative mode of $\hat{h}_{\rho_-}$. If one performs the numerical calculation, one finds that $\hat{h}_{\rho_-}$ has two negative modes, one of which is $2K$–periodic and the other $2K$–antiperiodic. Fig. 1 shows the k–dependence of the negative eigenvalues for $\theta = 1$. Since the $2K$–antiperiodic boundary condition is required for the proper continuum limit, we have to use the solid line in Fig. 1 as a negative eigenvalue. One should note that the negative eigenvalues approach zero in the small k region. We show in the following that this effect guarantees that the instanton–sphaleron transition in the small k–region is different from that in the large k–region. Fig. 2 shows normalized $2K$–antiperiodic eigenfunctions for the negative mode of $\hat{h}_{\rho_-}$ at ($\theta = 1$, $k = 0.6$) and ($\theta = 1$, $k = 0.99$).

We let $\psi_{-1}^{(\rho_-)}$ and $\epsilon_{-1}^{(\rho_-)}$ be respectively the $2K$–antiperiodic eigenfunction and corresponding eigenvalue for the negative mode. To obtain the criterion for the sharp first–order instanton–sphaleron transition we have to compute the nonlinear correction to the frequency

of the periodic instanton around the sphaleron. This can be carried out by solving Eq.(20) perturbatively. The perturbation procedure is briefly summarized in Appendix B. The criterion for the first-order transition is expressed as an inequality [6]

$$\Omega - \Omega_{sph} > 0, \tag{24}$$

where Ω is the frequency involving the nonlinear correction and $\Omega_{sph} \equiv \sqrt{-\epsilon_{-1}^{(\rho_-)}}$.

In Appendix B it is shown that the inequality (24) can be expressed as

$$< \psi_{-1}^{(\rho_-)} \mid D_1(z_1) > \quad < \quad 0 \tag{25}$$

where

$$D_1(z_1) = D_1^{(1)}(z_1) + D_1^{(2)}(z_1) + D_1^{(3)}(z_1). \tag{26}$$

Here

$$\begin{aligned} D_1^{(1)}(z_1) &= \frac{2\sqrt{2(1+k^2)}}{v}\psi_{-1}^{(\rho_-)}(z_1)\Bigg[k\left(v_1^2 + \frac{s_1(s_1+1)}{2}\right) sn[z_1] g_{\eta_1,1}(z_1) \\ &\qquad -\sqrt{s_1(s_1+1)}v_1 v_2 g'_{\eta_1,1}(z_1)\Bigg], \\ D_1^{(2)}(z_1) &= \frac{\sqrt{2(1+k^2)}}{v}\psi_{-1}^{(\rho_-)}(z_1)\Bigg[k\left(v_1^2 + \frac{s_1(s_1+1)}{2}\right) sn[z_1] g_{\eta_1,2}(z_1) \\ &\qquad -\sqrt{s_1(s_1+1)}v_1 v_2 g'_{\eta_1,2}(z_1)\Bigg], \\ D_1^{(3)}(z_1) &= \frac{3(1+k^2)}{4v^2}[v_1^4 + s_1(s_1+1)v_1^2 v_2^2]\psi_{-1}^{(\rho_-)3}(z_1), \end{aligned} \tag{27}$$

where $s_1 \equiv \sqrt{\theta^2 + \frac{1}{4}} - \frac{1}{2}$ and

$$\begin{aligned} g_{\eta_1,1}(z_1) &= \hat{h}_{\eta_1}^{-1} \mid q(z_1) >, \\ g_{\eta_1,2}(z_1) &= (\hat{h}_{\eta_1} + 4\Omega_{sph}^2)^{-1} \mid q(z_1) >, \\ \mid q(z_1) > \; &= -\frac{1}{v}\sqrt{\frac{1+k^2}{2}}\left[\theta\left((v_1 v_2)'\psi_{-1}^{(\rho_-)2} + 2v_1 v_2 \psi_{-1}^{(\rho_-)}\psi_{-1}^{(\rho_-)\prime}\right) + k(v_1^2 + \frac{\theta^2}{2}) sn[z_1]\psi_{-1}^{(\rho_-)2}\right]. \end{aligned} \tag{28}$$

It is now necessary to evaluate $g_{\eta_1,1}$ and $g_{\eta_1,2}$ explicitly. Although one can calculate $g_{\eta_1,1}$ exactly by following the procedure given in the Appendix of Ref. [18], this is not necessary

here. We already know the type of instanton–sphaleron transition at $k = 1$ [12,13] so that our interest concerns only the domain of small k. We can therefore adopt the following simple approximate procedure which has been shown to be valid in the small k region [18]. Using the completeness relation one can express $g_{\eta_1,1}$ as

$$g_{\eta_1,1} = \sum_{n=0}^{\infty} \frac{< \psi_n^{(\eta_1)} \mid q >}{\epsilon_n^{(\eta_1)}} \mid \psi_n^{(\eta_1)} > . \tag{29}$$

Since $\mid q >$ is an odd function, the zero mode of $\hat{h}_{\eta_1}$ does not contribute to the r.h.s. of Eq.(29). Hence the first approximation of $g_{\eta_1,1}$ is

$$g_{\eta_1,1} \approx \frac{< \psi_1^{(\eta_1)} \mid q >}{\epsilon_1^{(\eta_1)}} \mid \psi_1^{(\eta_1)} > \tag{30}$$

which can be evaluated numerically. In fact, this approximation is valid when $\mid \psi_1^{(\eta_1)} >$ is an isolated discrete mode and the density of higher states is very dilute. Ref. [18] shows these conditions are fulfilled in the small k–region if $\hat{h}_{\eta_1}$ is a Lam$\acute{e}$ operator as is the case here. In the same way $g_{\eta_1,2}$ is approximately

$$g_{\eta_1,2} \approx \frac{< \psi_1^{(\eta_1)} \mid q >}{3k^2 + 4\Omega_{sph}^2} \mid \psi_1^{(\eta_1)} > . \tag{31}$$

Fig. 3 shows the k-dependence of $J_i \equiv < \psi_{-1}^{(\rho_-)} \mid D_1^{(i)} >$ and $J_1 + J_2 + J_3$ at $\theta = 1$. Fig. 3 shows that the sharp first-order instanton-sphaleron transition occurs at $k < k_c \approx 0.2$ at $\theta = 1$. Although the result is not included in this paper, we have checked also the $\theta = 3$ case and have found a similar behavior: a sharp transition occurs in the small k region.

In conclusion we can say, we have found the sharp first–order instanton–sphaleron transition in the abelian–Higgs model in the small k region. Hence, depending on k, this model allows both smooth second–order transitions in the large k region and sharp first–order transitions in the small k region. These findings are similar to those of $d = 4$ SU(2)–Higgs theory in which the type of transition depends on the ratio of M_H and M_W.

Acknowledgement: This work has been supported by the Korea Research Foundation(1999-015-DP0074).

REFERENCES

[1] N. S. Manton, Phys. Rev. **D28**, 2019 (1983).

[2] F. Klinkhamer and N. S. Manton, Phys. Rev. **D30**, 2212, (1984).

[3] S. Y. Khnebnikov, V. A. Rubakov and P. Tinyakov, Nucl. Phys. **B367**, 334 (1991).

[4] E. Mottola and A. Wipf, Phys. Rev. **D39**, 588 (1989).

[5] S. Habib, E. Mottola and P. Tinyakov, Phys. Rev. **D54**, 7774 (1996).

[6] D. K. Park, H. Kim and S. Y. Lee, Nucl. Phys. **B557**, 146 (1999).

[7] G. Bonini, S. Habib, E. Mottola, C. Rebbi, R. Singleton and T. Tinyakov, hep-ph/9905243.

[8] K. L. Frost and L. G. Yaffe, Phys. Rev. **D59**, 06513 (1999); *ibid* **D60**, 105021 (1999).

[9] H. B. Nielsen and P. Olesen, Nucl. Phys. **B61**, 45 (1973).

[10] A. I. Bochkarev and M. E. Shaposhnikov, Mod. Phys. Lett. **A2**, 991 (1987).

[11] A. Kuznetsov and P. Tinyakov, Phys. Lett. **B406**, 76 (1997).

[12] V. V. Matveev, Phys. Lett. **B304**, 291 (1993).

[13] D. K. Park, H. J. W. Müller-Kirsten and J.–Q. Liang, hep-th/9910166.

[14] D. K. Park, S. Y. Lee and H. S. Kim, Phys. Lett. **B463**, 206 (1999).

[15] L. Carson, Phys. Rev. **D42**, 2853 (1990).

[16] By the period of the sphaleron we mean the period of the periodic instanton solution when it approches the sphaleron.

[17] F.M. Arscott, *Periodic Differential Equations* (Pergamon, 1964).

[18] D. K. Park, H. J. W. Müller-Kirsten and J.–Q. Liang, hep-th/9910151, to appear in Nucl. Phys. B.

Appendix A

Here we explain how the spectrum of $\hat{h}_{\rho_-}$ is obtained. The spectrum of $\hat{h}_{\rho_+}$ can be obtained similarly. The eigenvalue equation of $\hat{h}_{\rho_-}$ is

$$\left[-\frac{\partial^2}{\partial z_1^2} + f(k,\theta,z_1)\right]\psi_n^{(\rho_-)} = \zeta\psi_n^{(\rho_-)} \tag{32}$$

where

$$f(k,\theta,z_1) = (1+\theta^2)k^2 sn^2[z_1] - \sqrt{(1+4\theta^2)\left(k^2 sn^2[z_1] - \frac{1+k^2}{2}\right)^2 - \theta^2(1-k^2)^2}, \tag{33}$$

$$\zeta = \epsilon^{(\rho_-)} + \frac{1+k^2}{2}.$$

We first choose the $4K$–periodic boundary condition. In this case we can use the Fourier expansions

$$f(k,\theta,z_1) = \sum_{n=-\infty}^{\infty} a_n e^{i\frac{n\pi}{l}z_1}, \tag{34}$$

$$\psi_n^{(\rho_-)} = \sum_{n=-\infty}^{\infty} b_n e^{i\frac{n\pi}{l}z_1},$$

where $l = 2K$ and the coefficient a_n is given by

$$a_n = \frac{1}{2l}\int_{-l}^{l} f(k,\theta,z_1)e^{-i\frac{n\pi}{l}z_1}. \tag{35}$$

Inserting (34) into (32) and using the property of linear independence of the exponential function one obtains

$$\sum_m \left[\left(\frac{n\pi}{l}\right)^2 \delta_{mn} + a_{n-m}\right] b_m = \zeta b_n. \tag{36}$$

Solving this matrix equation numerically, one can evaluate the eigenvalue $\epsilon_n^{(\rho_-)}$ and eigenfunction $\psi_n^{(\rho_-)}$. After that we choose only $2K$–antiperiodic eigenfunctions and determine the corresponding eigenvalues for the proper $k = 1$ limit.

Appendix B

In this appendix we show briefly how the inequality (25) is derived for the criterion of the sharp first–order transition by solving Eq.(20) perturbatively. First we choose an *ansatz*

$$\begin{pmatrix} a_0 \\ \rho_+ \\ \rho_- \\ \eta_1 \end{pmatrix} = \Delta \begin{pmatrix} a_{0,0}(z_1) \\ \rho_{+,0}(z_1) \\ \rho_{-,0}(z_1) \\ \eta_{1,0}(z_1) \end{pmatrix} \cos \Omega_{sph} z_0 \tag{37}$$

where Δ is a small oscillation amplitude around the sphaleron. After inserting (37) into Eq.(20) and neglecting higher order terms, one obtains

$$\begin{aligned} \Omega_{sph} &= \sqrt{-\epsilon_{-1}^{(\rho_-)}}, \\ a_{0,0} &= 0, \qquad\qquad \rho_{+,0} = 0, \\ \rho_{-,0} &= \psi_{-1}^{(\rho_-)}, \qquad\qquad \eta_{1,0} = 0. \end{aligned} \tag{38}$$

For the next order perturbation we set

$$\begin{pmatrix} a_0 \\ \rho_+ \\ \rho_- \\ \eta_1 \end{pmatrix} = \begin{pmatrix} \Delta^2 a_{0,1}(z_0, z_1) \\ \Delta^2 \rho_{+,1}(z_0, z_1) \\ \Delta \rho_{-,0}(z_1) \cos \Omega z_0 + \Delta^2 \rho_{-,1}(z_0, z_1) \\ \Delta^2 \eta_{1,1}(z_0, z_1) \end{pmatrix}. \tag{39}$$

Inserting Eq.(39) into Eq.(20) and considering only terms up to those of quadratic order, one can show there is no frequency shift to this order. It is also straightforward to show that $a_{0,1} = 0$, $\rho_{+,1} = 0$, $\rho_{-,1} = 0$, and

$$\eta_{1,1} = g_{\eta_1,1}(z_1) + g_{\eta_1,2}(z_1) \cos 2\Omega_{sph} z_0 \tag{40}$$

where $g_{\eta_1,1}$ and $g_{\eta_1,2}$ are given by Eq.(28).

For the next order perturbation we set

$$\begin{pmatrix} a_0 \\ \rho_+ \\ \rho_- \\ \eta_1 \end{pmatrix} = \begin{pmatrix} \Delta^3 a_{0,2}(z_0, z_1) \\ \Delta^3 \rho_{+,2}(z_0, z_1) \\ \Delta \rho_{-,0}(z_1) \cos \Omega z_0 + \Delta^3 \rho_{-,2}(z_0, z_1) \\ \Delta^2 \eta_{1,1}(z_0, z_1) + \Delta^3 \eta_{1,2}(z_0, z_1) \end{pmatrix}. \tag{41}$$

Inserting this into Eq.(20) and considering contributions up to those of cubic order, one can show that there is a frequency change in this order given by

$$\Omega_{sph}^2 - \Omega^2 = \Delta^2 < \rho_{-,0} \mid D_1 > \tag{42}$$

which proves Eq.(25).

TABLES

Eigenvalue of $\hat{h}_{\eta_1}$	Eigenfunction of $\hat{h}_{\eta_1}$
$\lambda_0^{(\eta_1)} = 0$	$\psi_0^{(\eta_1)}(z_1) = N_0 cn[z_1]dn[z_1]$
$\lambda_1^{(\eta_1)} = 3k^2$	$\psi_1^{(\eta_1)}(z_1) = N_1 sn[z_1]dn[z_1]$

FIGURES

FIG. 1. k-dependence of the negative eigenvalues $\epsilon^{(\rho-)}$ of $\hat{h}_{\rho-}$ at $\theta = 1$. The dotted line and the solid line represent the negative eigenvalues for the $2K$–periodic and $2K$–antiperiodic eigenfunctions respectively. For the correct $k = 1$ limit we have to choose the solid line as the negative eigenvalue.

FIG. 2. The normalized $2K$–antiperiodic eigenfunctions for the negative mode of $\hat{h}_{\rho-}$ at (a) $\theta = 1$, $k = 0.6$, and (b) $\theta = 1$, $k = 0.99$.

FIG. 3. k-dependence of J_1, J_2, J_3, and $J_1 + J_2 + J_3$ at $\theta = 1$. This shows that the sharp first–order instanton–sphaleron transition occurs at $k < k_c \approx 0.2$.

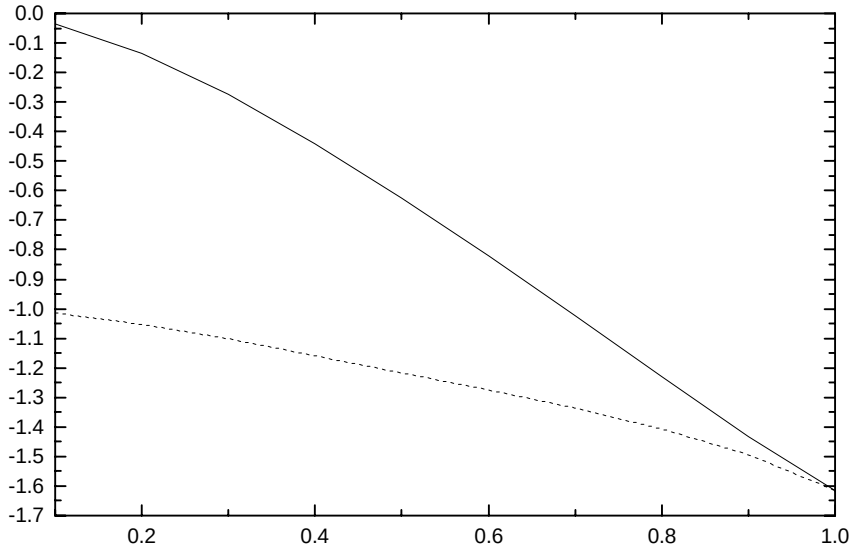

Fig. 1

θ = 1, k = 0.6

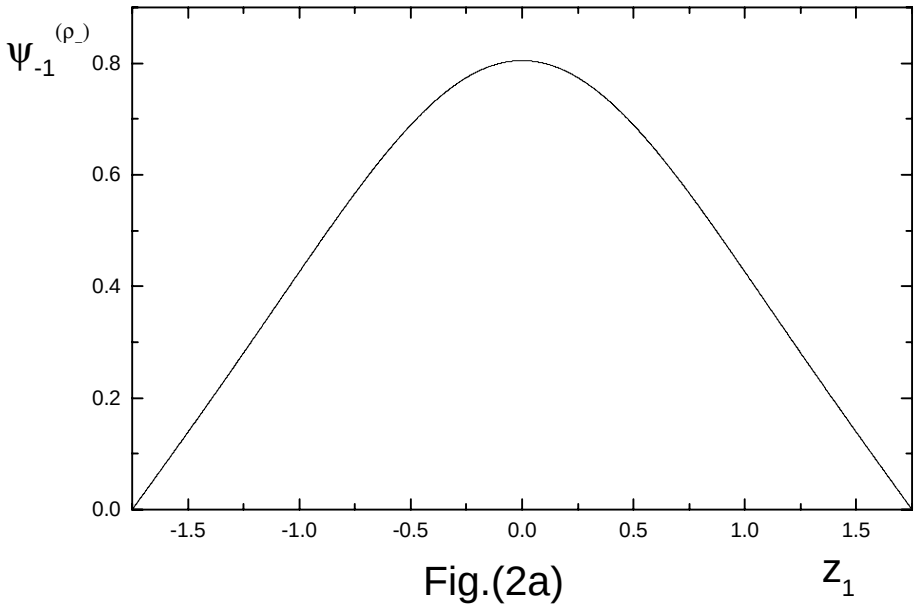

Fig.(2a)

θ = 1, k = 0.99

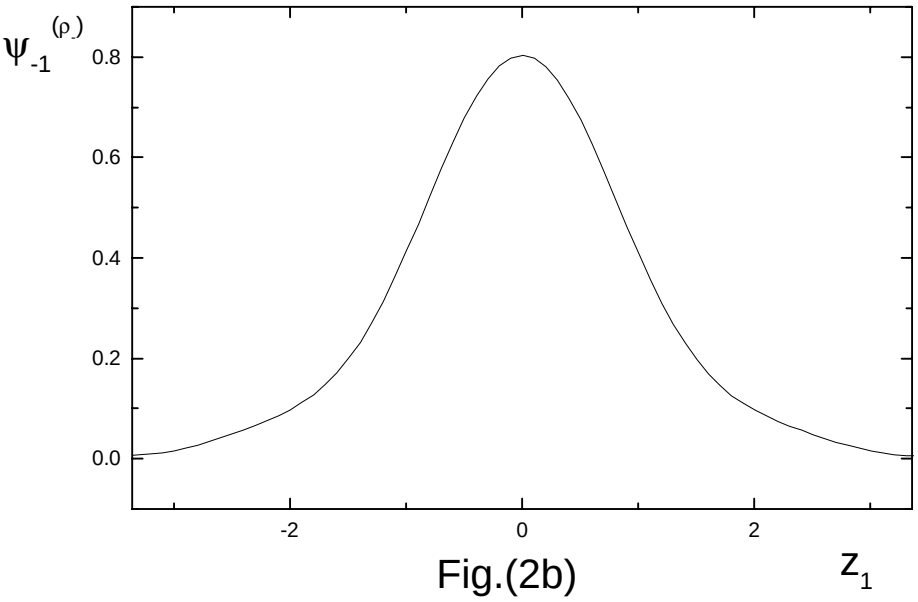

Fig.(2b)

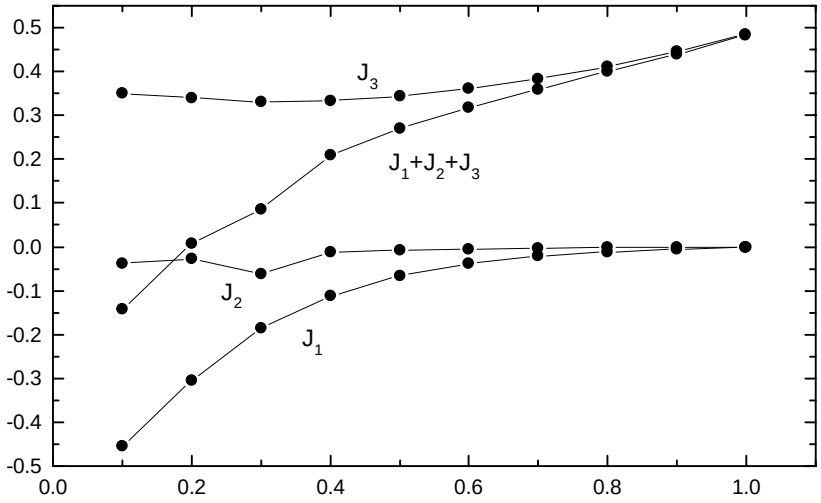

Fig. 3